

Supplemental Information

Gene Transfer with AAV9-PHP.B Rescues Hearing in a Mouse Model of Usher Syndrome 3A and Transduces Hair Cells in a Non-human Primate

Bence György, Elise J. Meijer, Maryna V. Ivanchenko, Kelly Tenneson, Frederick Emond, Killian S. Hanlon, Artur A. Indzhukulian, Adrienn Volak, K. Domenica Karavitaki, Panos I. Tamvakologos, Mark Vezina, Vladimir K. Berezovskii, Richard T. Born, Maureen O'Brien, Jean-François Lafond, Yvan Arsenijevic, Margaret A. Kenna, Casey A. Maguire, and David P. Corey

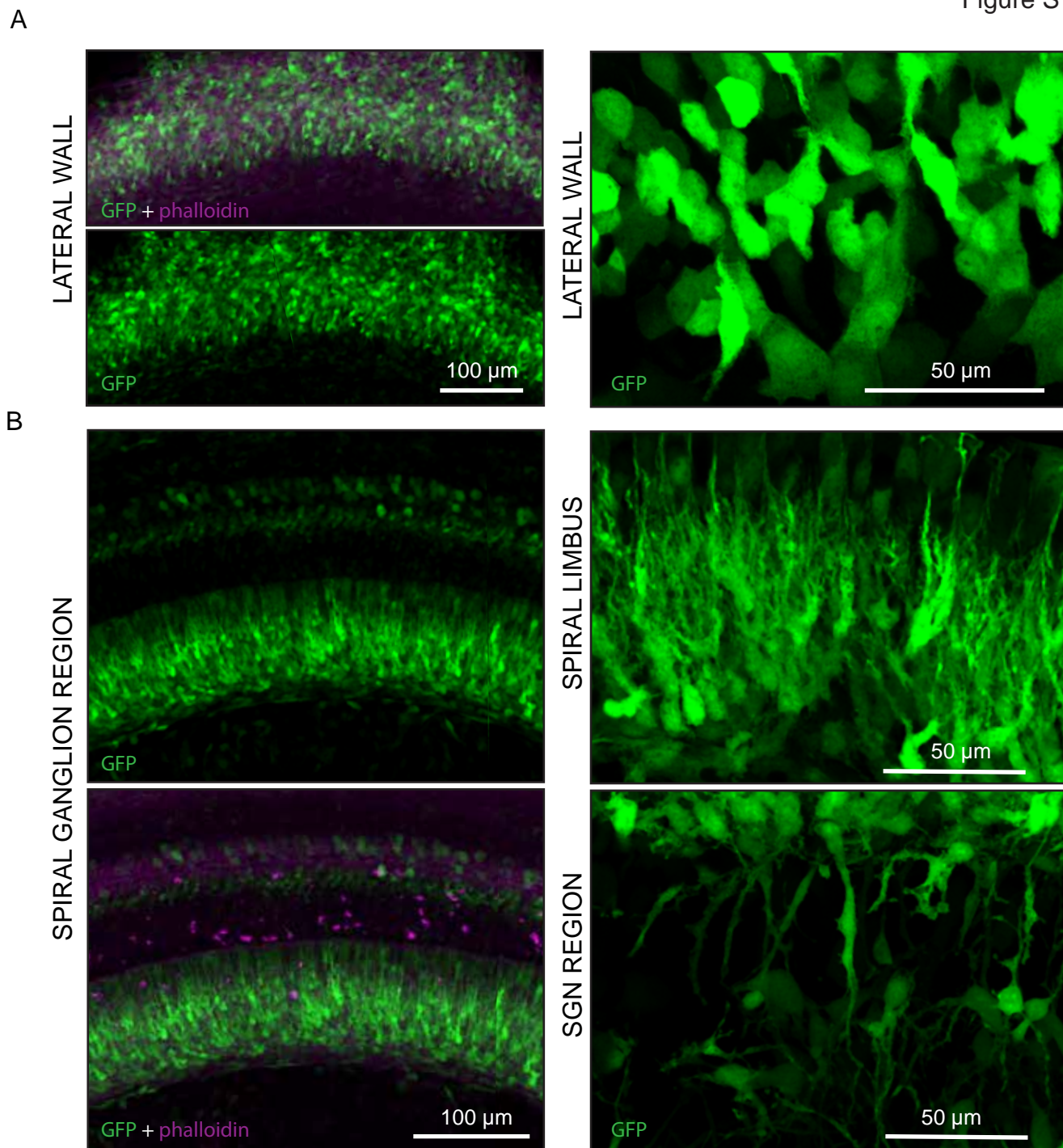


Figure S1. Transduction efficiency of AAV9-PHP.B-CBA-GFP in the lateral wall and spiral ganglion region of the cochlea, after neonatal RWM injection. (A) C57BL/6J mice were injected at P1 with 5×10^{10} vector genomes, cochleas were explanted at P5, and cultured for one more day (P5+1). Low magnification (left panel) and high magnification (right panel) images of the lateral wall. Left panel shows GFP together with phalloidin staining of actin (top) and GFP staining only (bottom); right panel shows GFP. (B) Low magnification images of spiral ganglion region (left) and high magnification images of spiral limbus and spiral ganglion neurons (SGN) region.

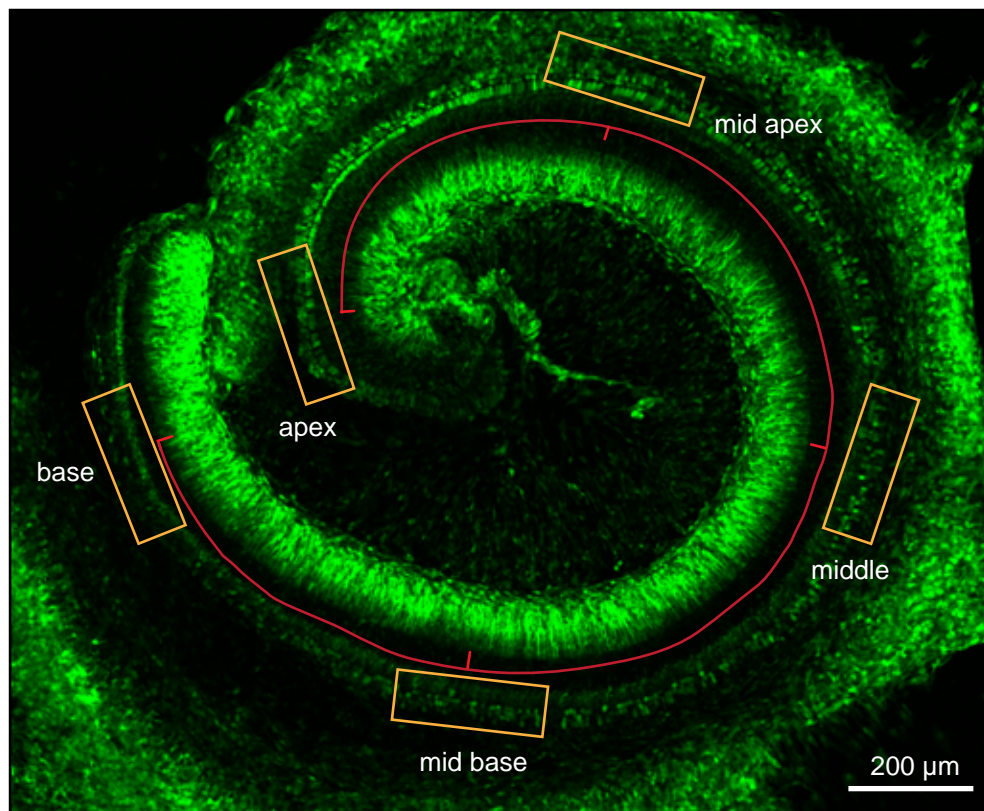


Figure S2. Quantification method for determination of transduction efficiency in specified cochlear regions. Transduction efficiencies in IHCs and OHCs were quantified in 5 different regions (apex, mid apex, middle, mid base, base (yellow boxes). The regions were ~800 μm apart from each other (red trace).

Right cochlea (non injected ear) WT (C57BL/6J)

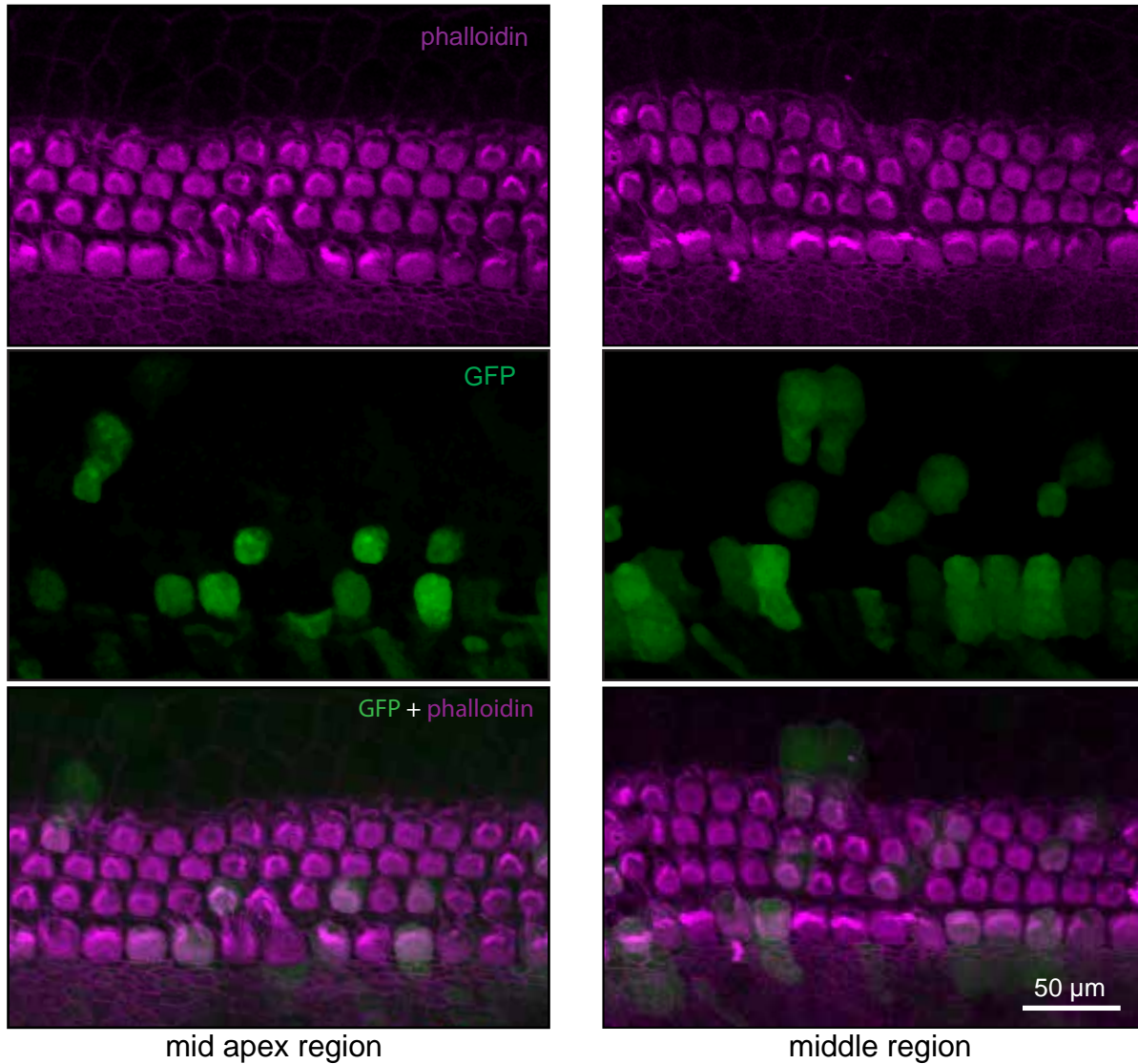


Figure S3. Transduction of AAV9-PHP.B-CBA-GFP in a non-injected ear of a C57BL/6J mouse after neonatal round window membrane (RWM) injection to the contralateral ear. Left panels (mid apex region) and right panels (middle region) show GFP expression in some IHCs and OHC.

Adult injection (C57BL/6J)

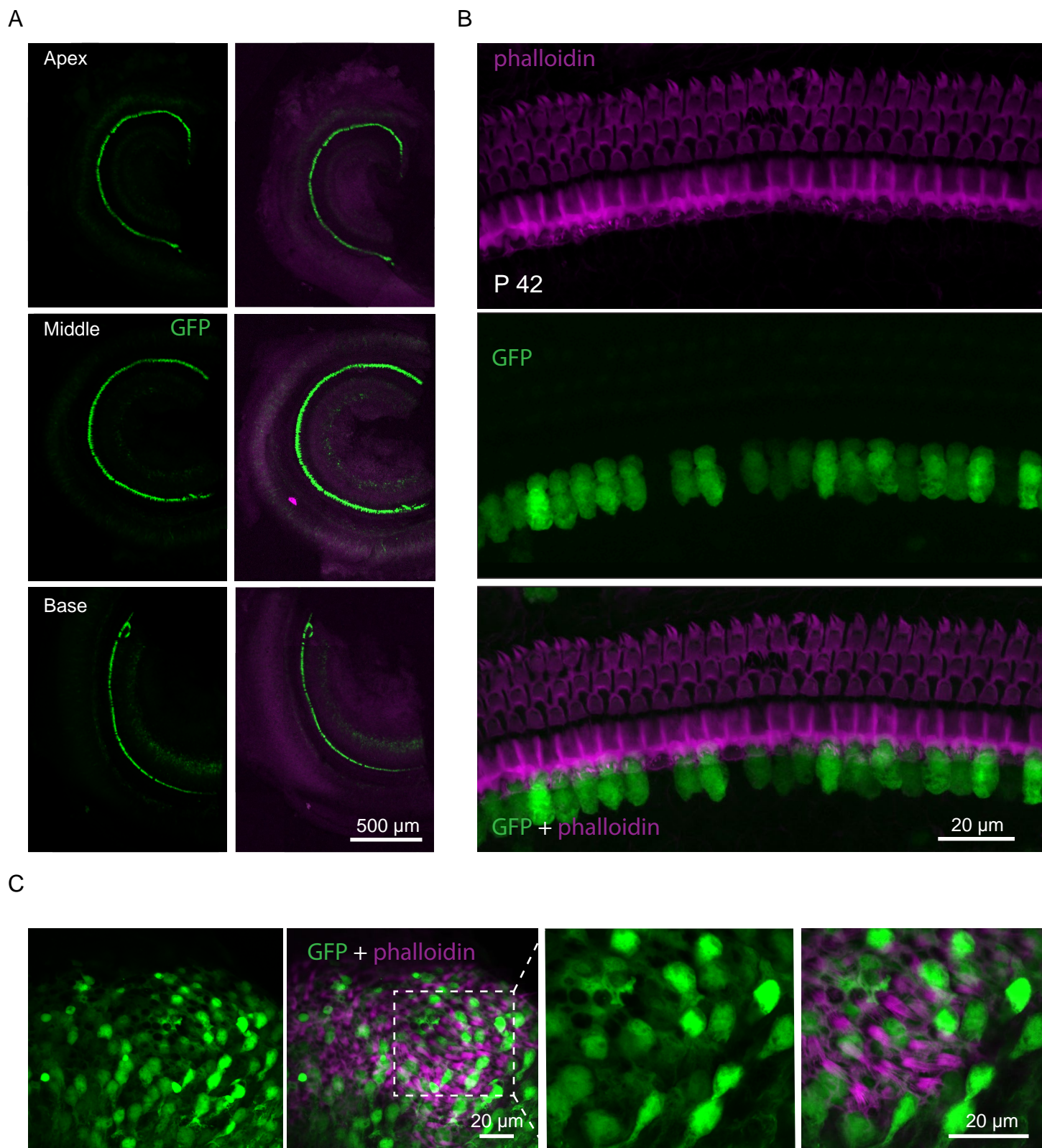
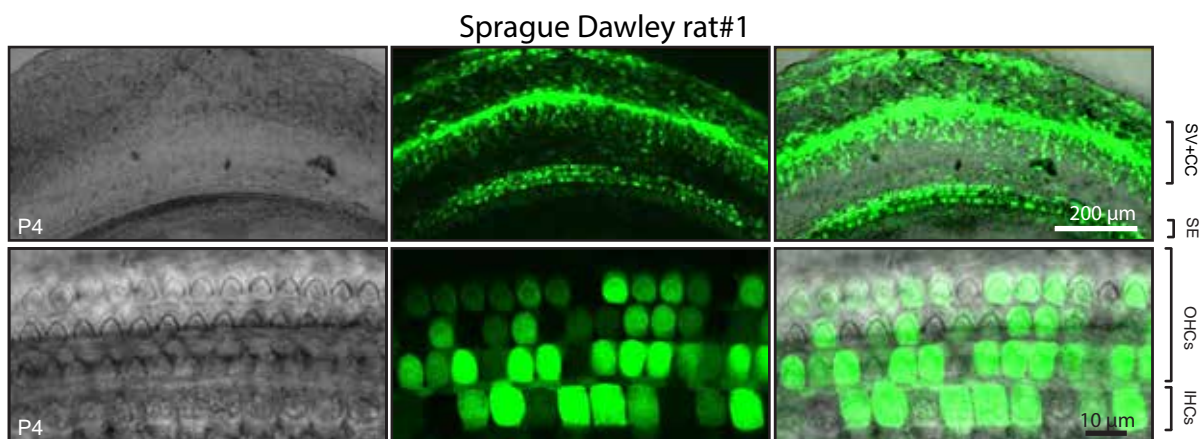


Figure S4. Transduction of adult hair cells by AAV9-PHP.B-CBA-GFP in C57BL/6J mice after injection at P28 through the posterior semicircular canal. Four-week old animals were injected with 2×10^{10} vector genomes. At P42 (2 weeks after injection), transduction was observed in almost all IHCs, but not in OHCs. **(A)** Low magnification images of the apical, middle and basal turns of the cochlea. **(B)** High magnification images of middle region of the cochlea with the high transduction in the IHCs. **(C)** AAV9-PHP.B-CBA-GFP transduces cells in the vestibular system (utricle).

A



B

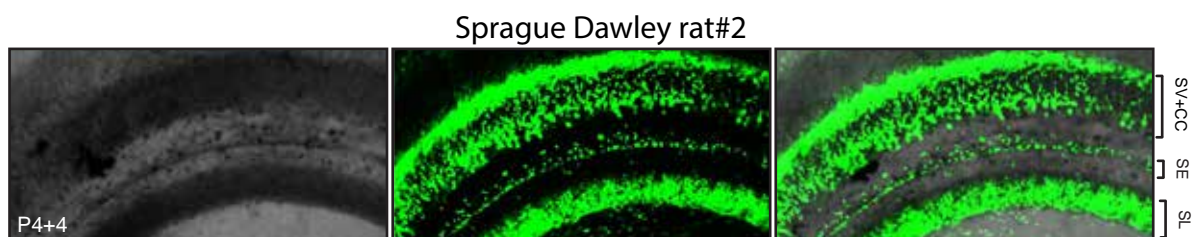


Figure 5. Transduction efficiency in Sprague Dawley rats of AAV9-PHP.B-CBA-GFP after neonatal RWM injection. Transduction efficiency of AAV9-PHP.B-CBA-GFP after neonatal round window membrane injection in rat#1 and rat#2 (**A**, **B**). Live cell imaging was performed in explanted cochleas at P4 for the rat#1 (**A**) and P4+4 days in culture for the rat #2 (**B**). Lower magnification images are shown on the top (**A**, **B**) and higher magnification at the bottom (**A**). Left panels show DIC imaging to visualize hair bundles.

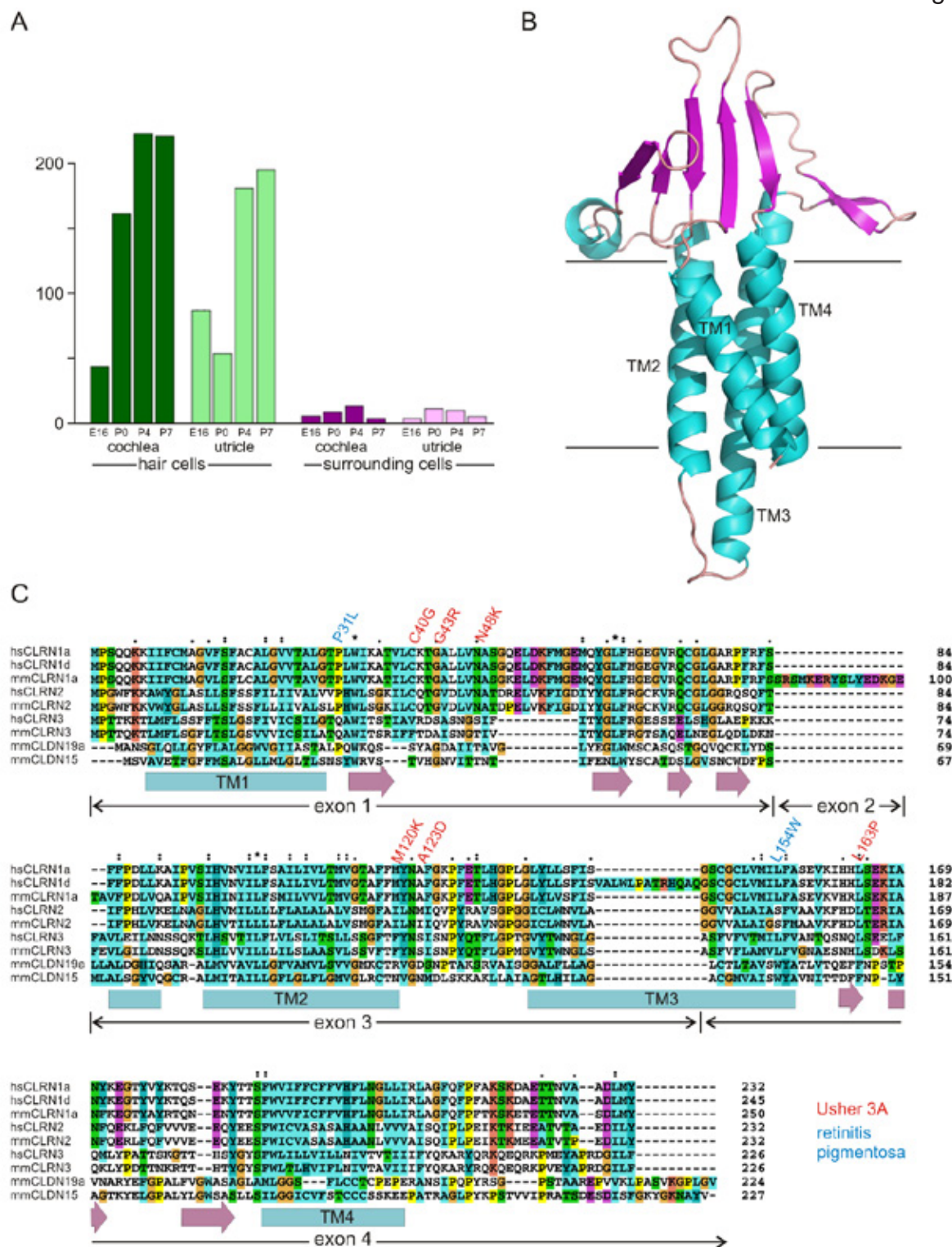


Figure S6. Expression, predicted structure and sequence alignment for CLRN1-related proteins. (A) Expression of *Clrn1* in mouse inner ear, from Scheffer et al. (2015). mRNA levels rise around the time that hair cells gain mechanosensitivity, but there is little expression in surrounding cells. (B) Predicted structure of hsCLRN1 based on known structures of CLDN19 and CLDN15 (Phyre2; Kelly et al., 2015). (C) Alignment of human and mouse CLRN1 splice forms with mouse CLDN19 and CLDN15. Mutations in hsCLRN1 producing Usher syndrome 3A or retinitis pigmentosa alone are indicated.

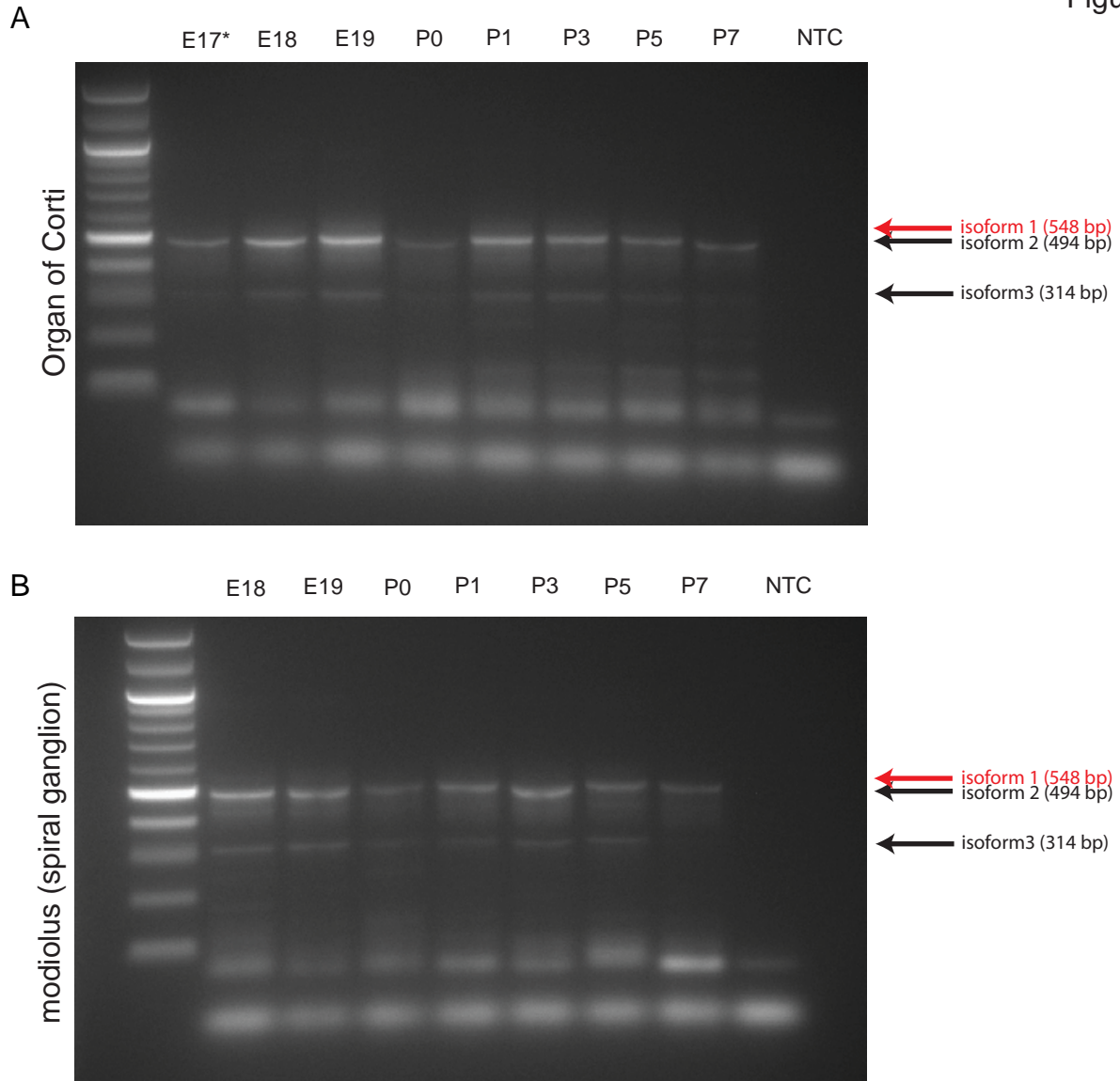


Figure S7. Clarin-1 expression and isoform analysis from E17 to P7. RNA was isolated from from the organ of (A) Corti region and (B) spiral ganglion region at different stages of development. Whole cochlea was used at E17. RT-PCR was performed using primers in exon 1 and exon 4. PCR products were run on a 1% agarose gel. Isoforms and sizes are shown on the right. For size comparison, we used a 100bp ladder from NEB.

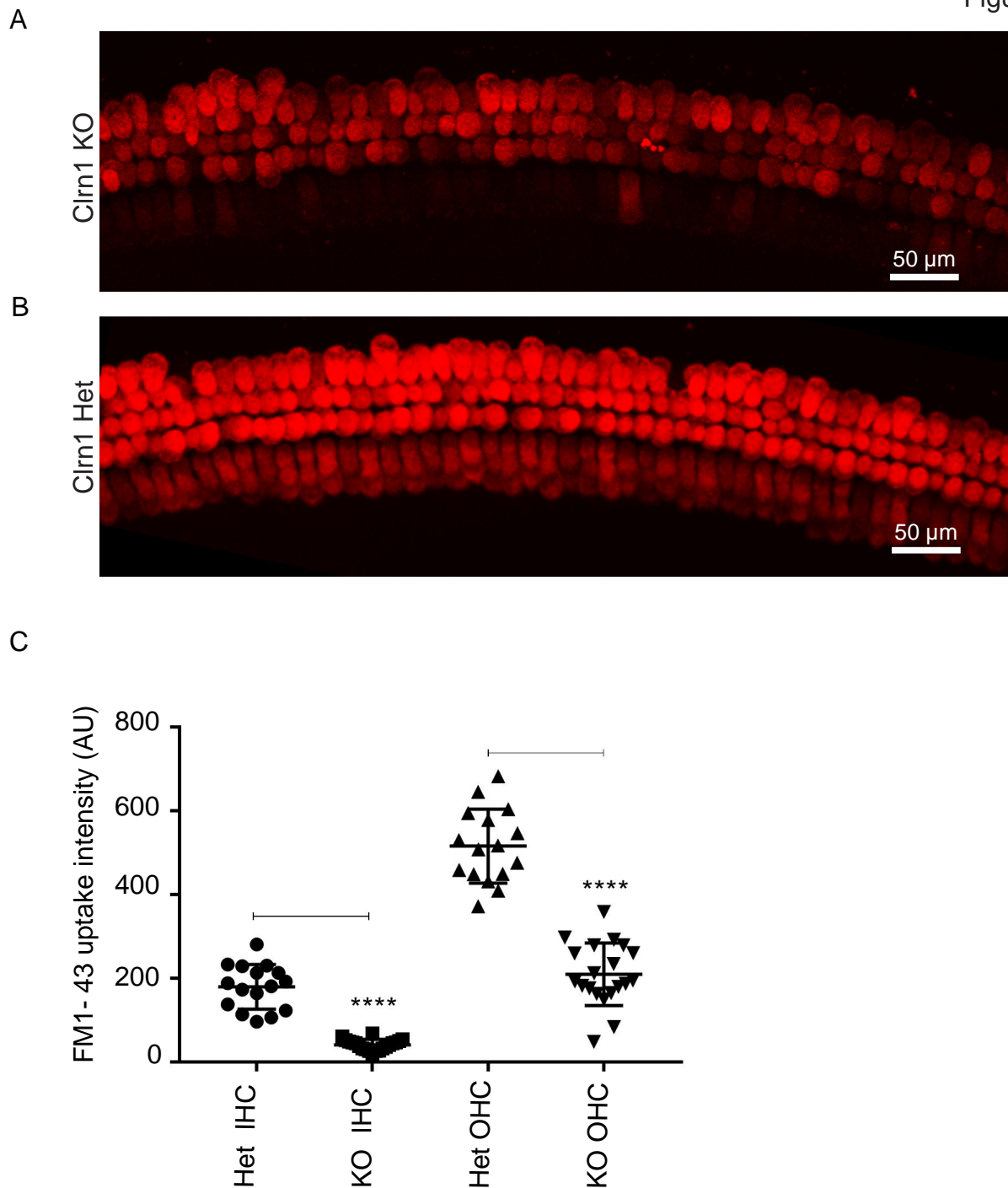


Figure S8. FM1-43 loading in hair cells from Clnr1 heterozygous (Het) and homozygous (KO) knockout mice. (A, B) Confocal microscopy images of FM1-43-loaded hair cells in KO and Het mice. (C) FM1-43 signal intensity measured with ImageJ. In Clnr1 KO mice, FM1-43 intensity was significantly lower than in heterozygotes, in both IHCs and OHCs. Unpaired t-test for all regions combined; $p < 0.0001$ for both IHCs and OHCs.

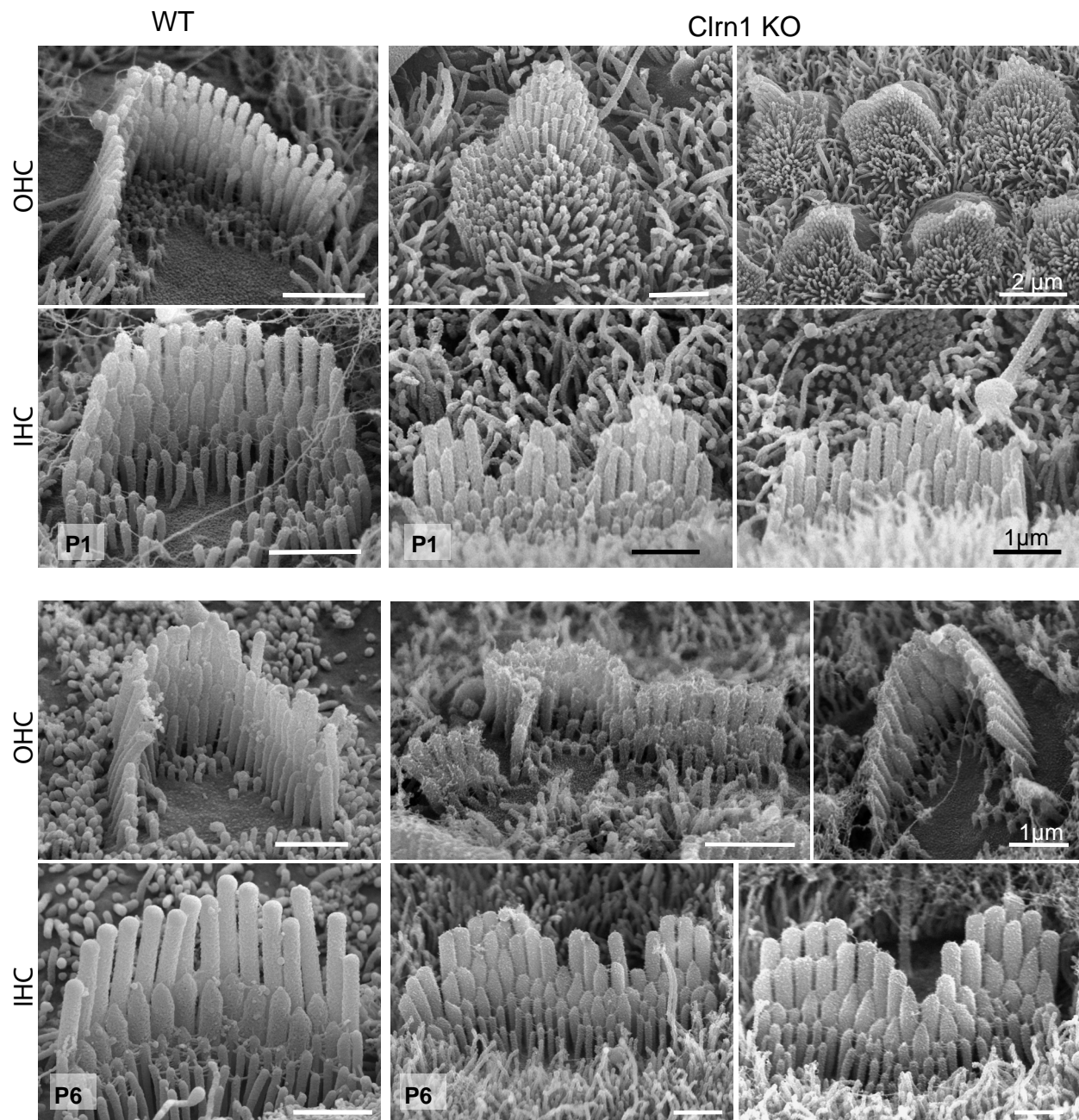


Figure S9. SEM images of organ of Corti from mid-cochlear regions, from WT and *Cln1* KO mice. SEM analysis of *Cln1* KO revealed loss of orientation and disorganization of hair bundles compared to the WT hair cells at, beginning as early as P1 and progressing at P6, with separation of columns, missing and shortened stereocilia, and distorted tips.

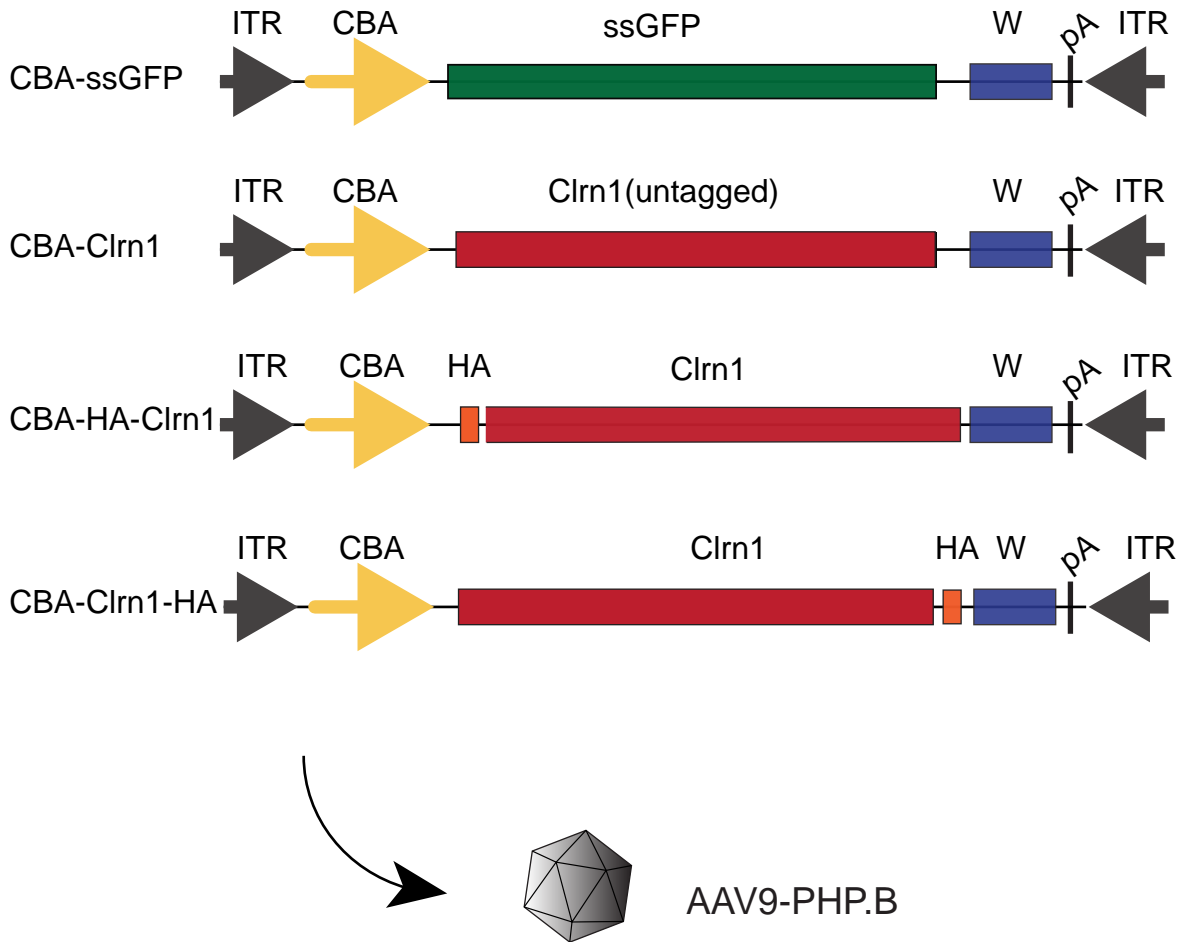


Figure S10. Schematics of the AAV vectors used in the study. From top: GFP vector, untagged clarin-1 vector, N-terminal HA-tagged clarin-1 vector, and C-terminal HA-tagged clarin-1 vector. All vectors are single stranded. ITR: inverted terminal repeat, CBA: chicken beta-actin promoter, HA: hemagglutinin tag, W: WPRE element (woodchuck hepatitis virus posttranscriptional regulatory element), pA: BGH poly A signal.

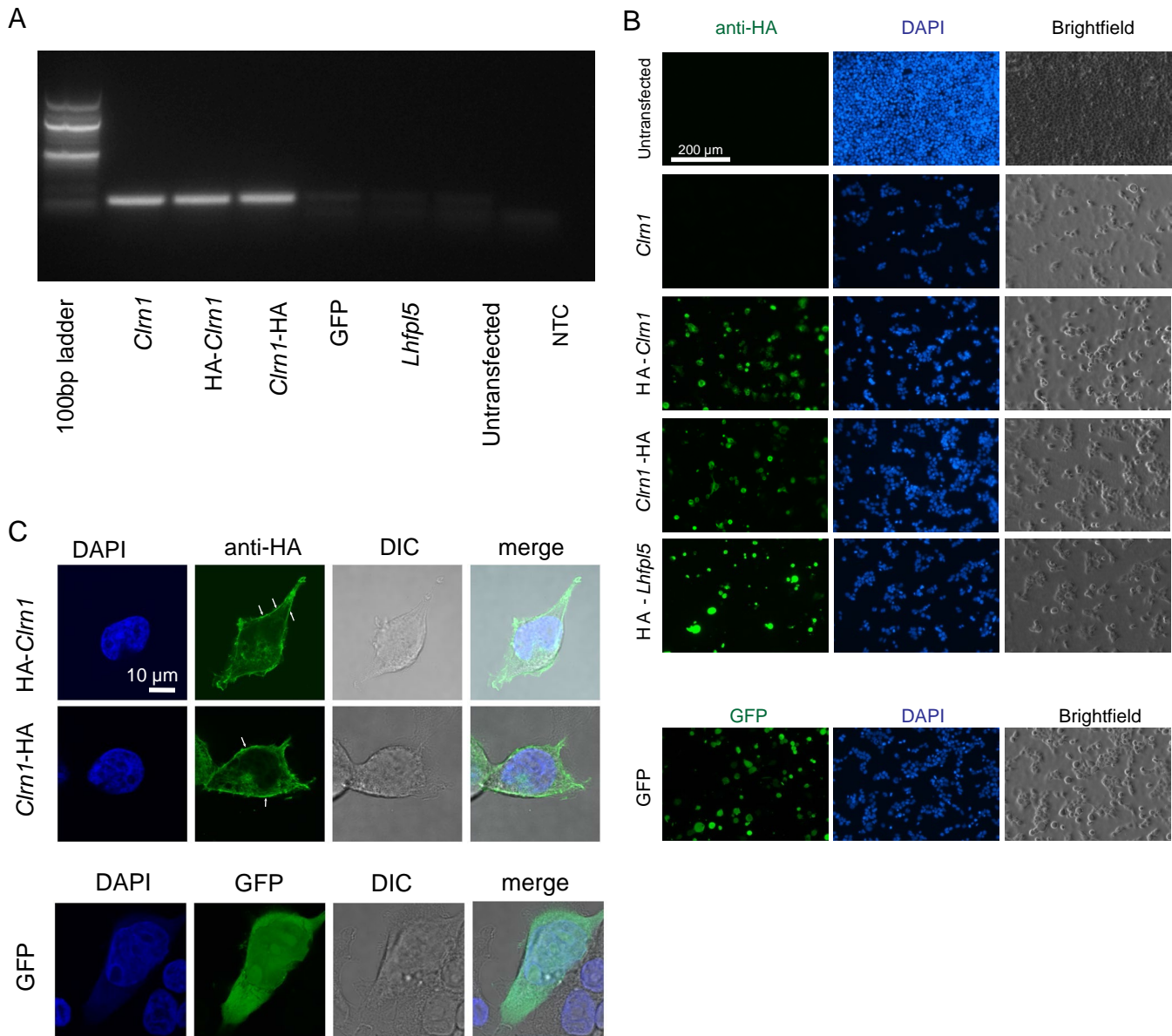
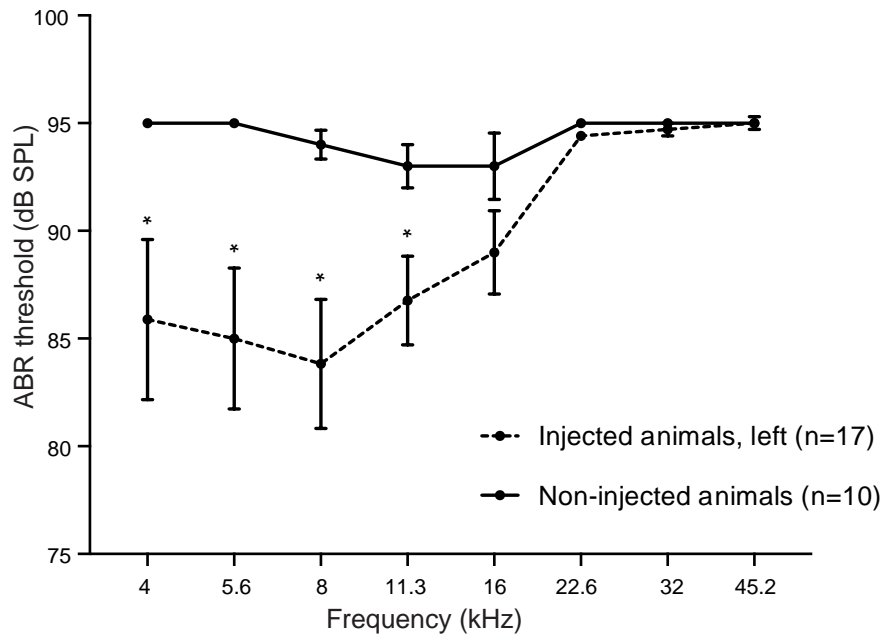


Figure S11. Clarin-1 expression in HEK cells. Cells were transfected with CBA-*Clrn1*, CBA-HA-*Clrn1*, CBA-*Clrn1*-HA, CBA-GFP and CBA-HA-*Lhfp15* AAV plasmids. (A) RT-PCR products were run on a 1% agarose gel; expected product size is 171 bp. (B) Immunostaining for HA or native GFP fluorescence. (C) High magnification confocal images; HA staining or GFP fluorescence.

A Cln1 KO, 4 weeks, AAV.PHP.B-CBA-Cln1 injected vs non-injected



B

Cln1 KO, 4 weeks, AAV.PHP.B-CBA-Cln1 injected, left vs right

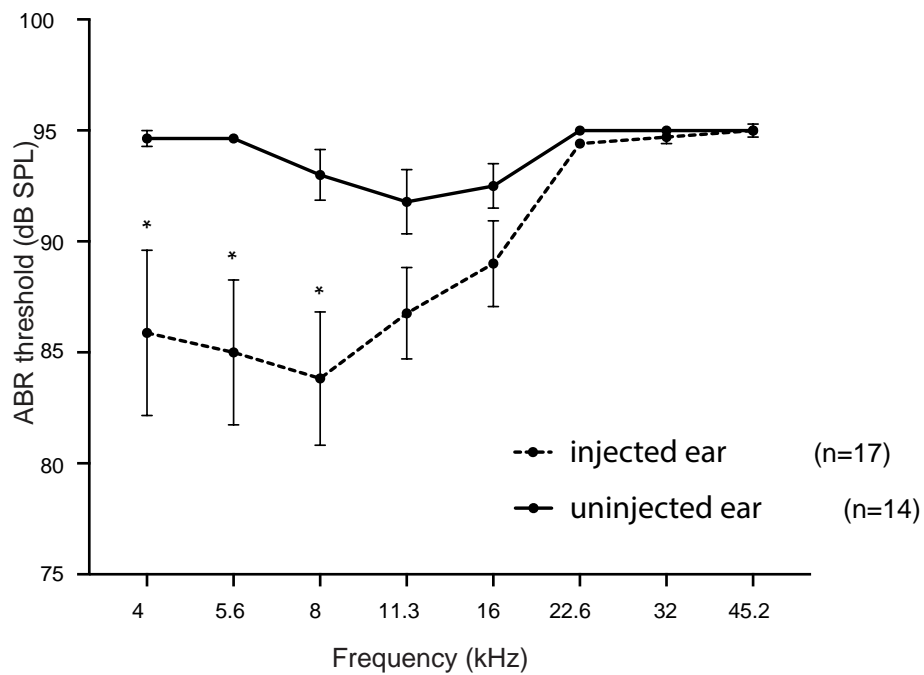
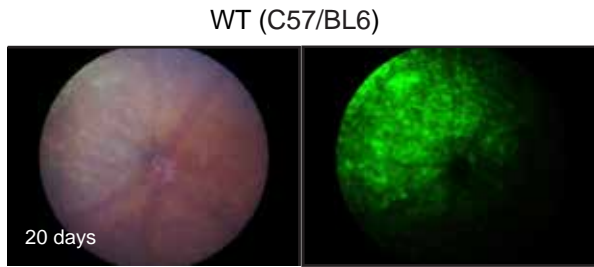


Figure S12. AAV9-PHP.B-Clarín mediated rescue of hearing in Cln1 KO animals is significantly better than (A) non-injected mice and (B) injected ear (left) vs. uninjected (right) ear. Both (A) and (B) are from the same data described in Figure 3. $p < 0.05$, Wilcoxon test.

A



B

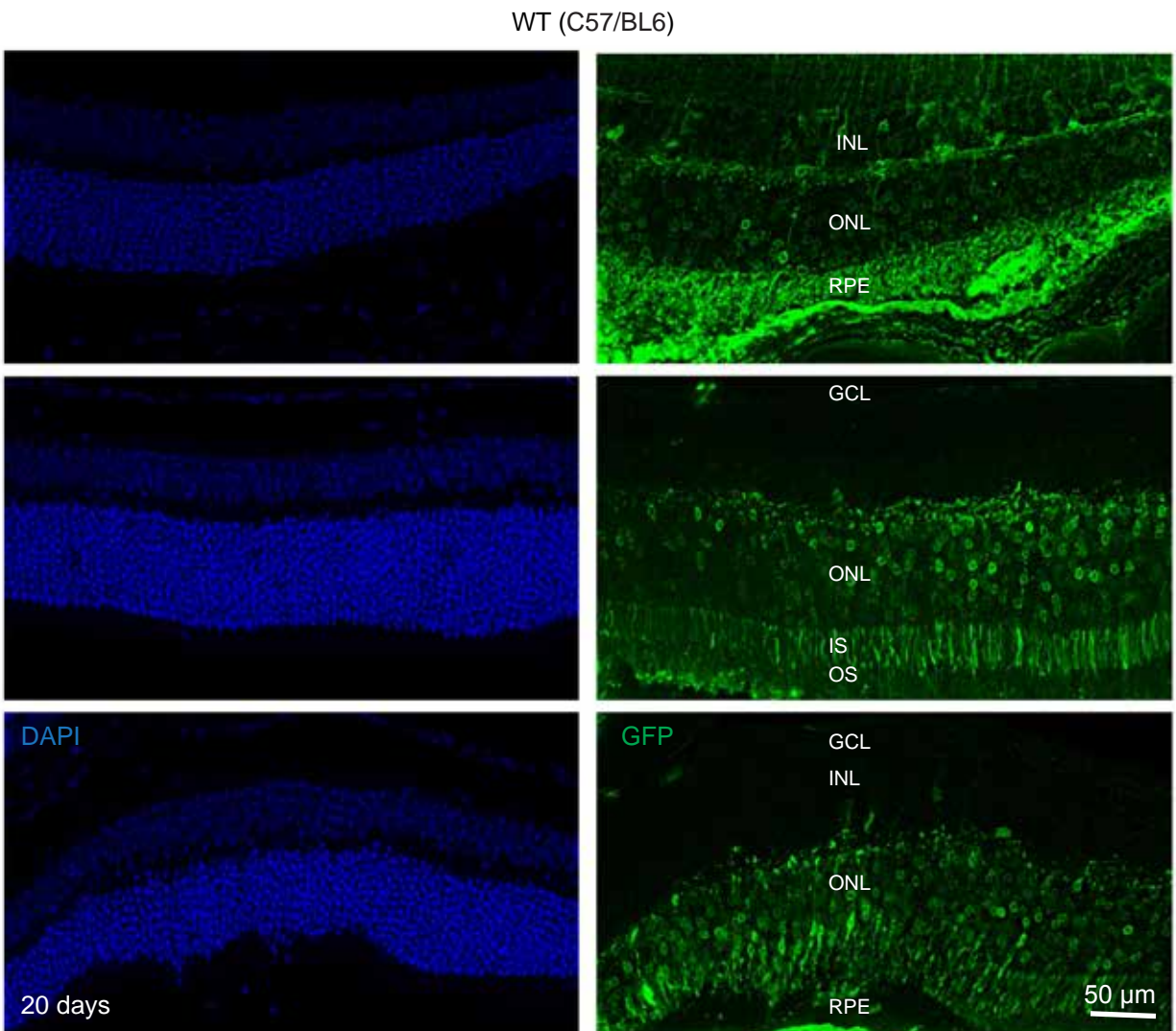


Figure S13. Transduction of mouse retina with AAV9-PHP.B-CBA-GFP. Adult (4.5 months) C57/BL6 mice were injected subretinally with AAV9-PHP.B-CBA-GFP (2.1×10^9 vg contained in 1μ l). (A) Many retinal cells were transduced after 20 days post injection. (B) Numerous photoreceptors were GFP-positive GCL: ganglion cell layer, INL: inner nuclear layer; ONL: outer nuclear layer; RPE, retinal pigment epithelium.

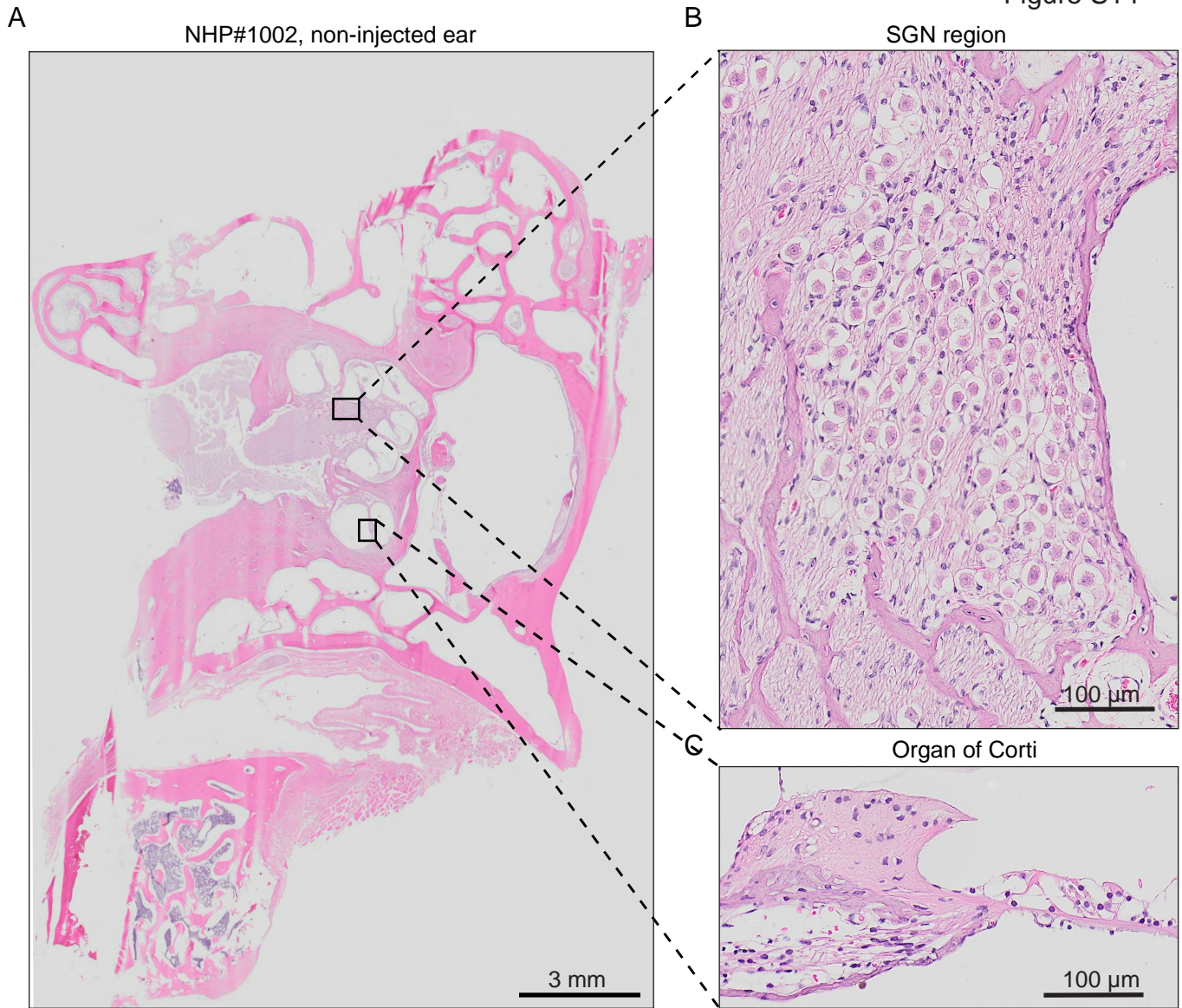


Figure S14. Hematoxylin and Eosin staining of the non-injected ear of Cynomolgus monkey #1002. (A) A low magnification image is shown with areas of interest indicated by rectangles. Magnified image of spiral ganglion neurons (SGN) region (B) and organ of Corti (C).

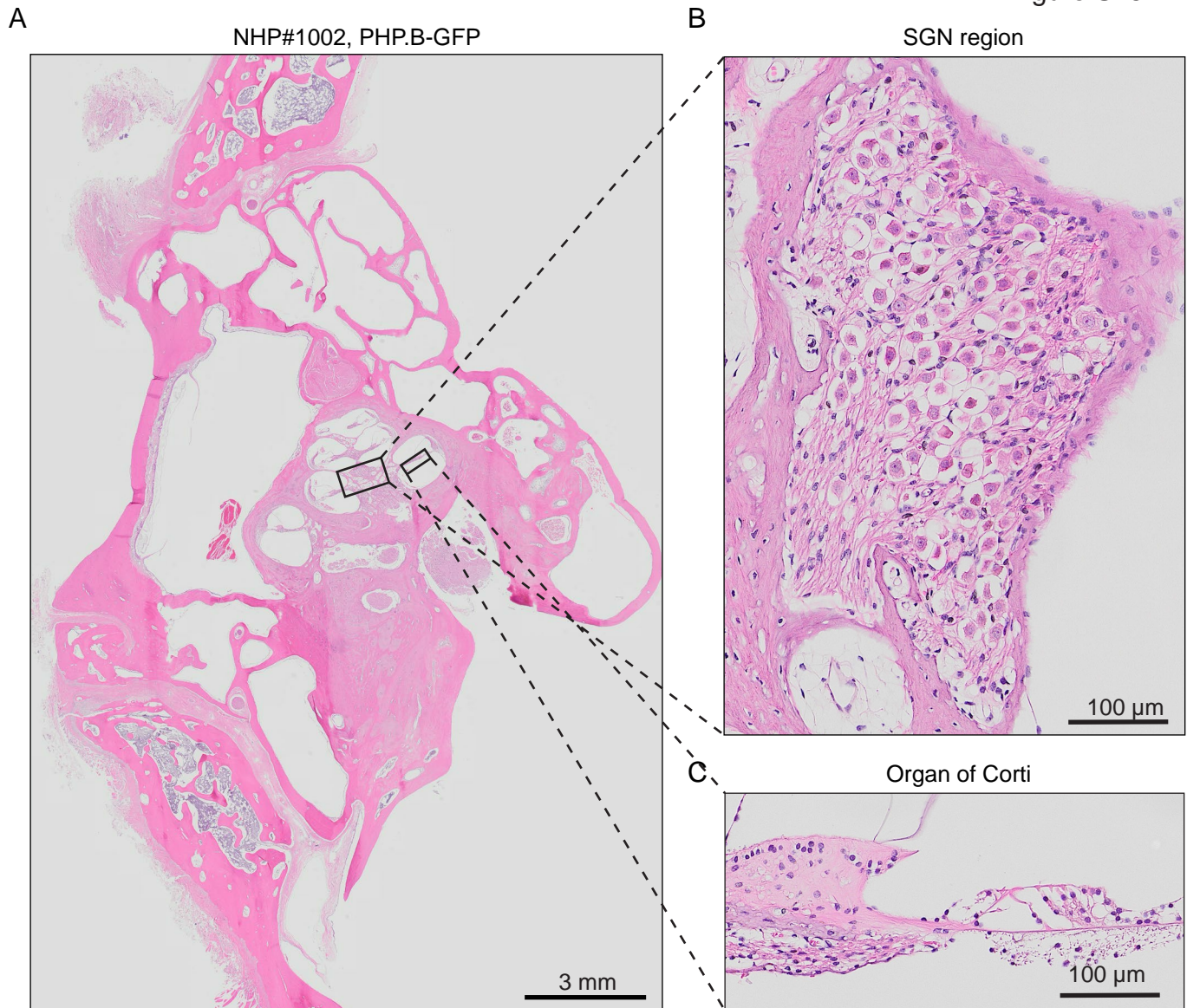


Figure S15. Hematoxylin and Eosin staining of the AAV9-PHP.B-CBA-GFP (3×10^{11} VG) injected ear of Cynomolgus monkey #1002. (A) A low magnification image is shown with areas of interest indicated by rectangles. Magnified image of spiral ganglion neurons (SGN) region (B) and organ of Corti (C) show normal cellular morphology.

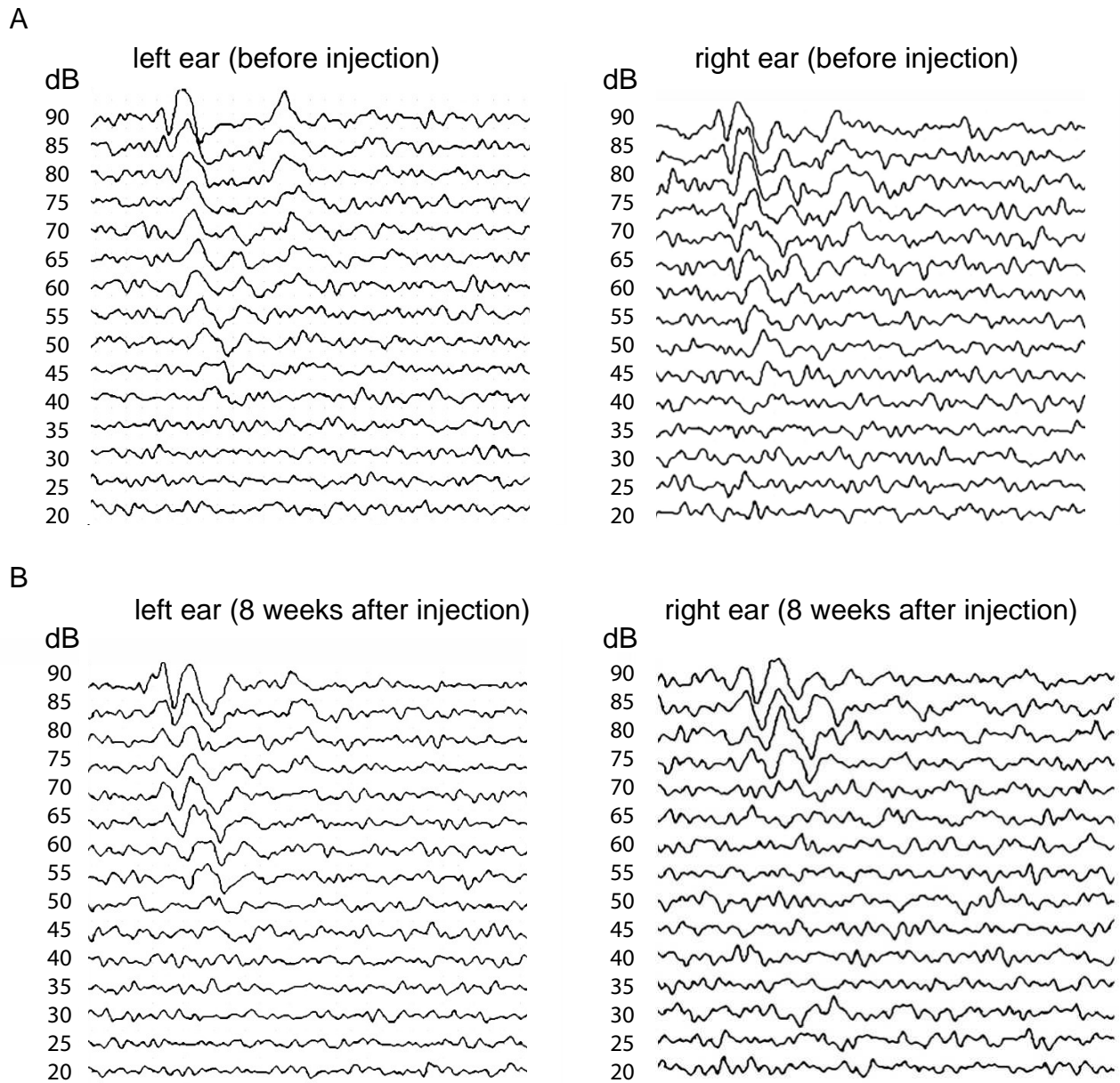


Figure S16. ABR test of Cynomolgus monkey #3501 injected with AAV9-PHP.B-CBA-GFP (1×10^{11} VG) before (A) and 8 weeks after injection (B).

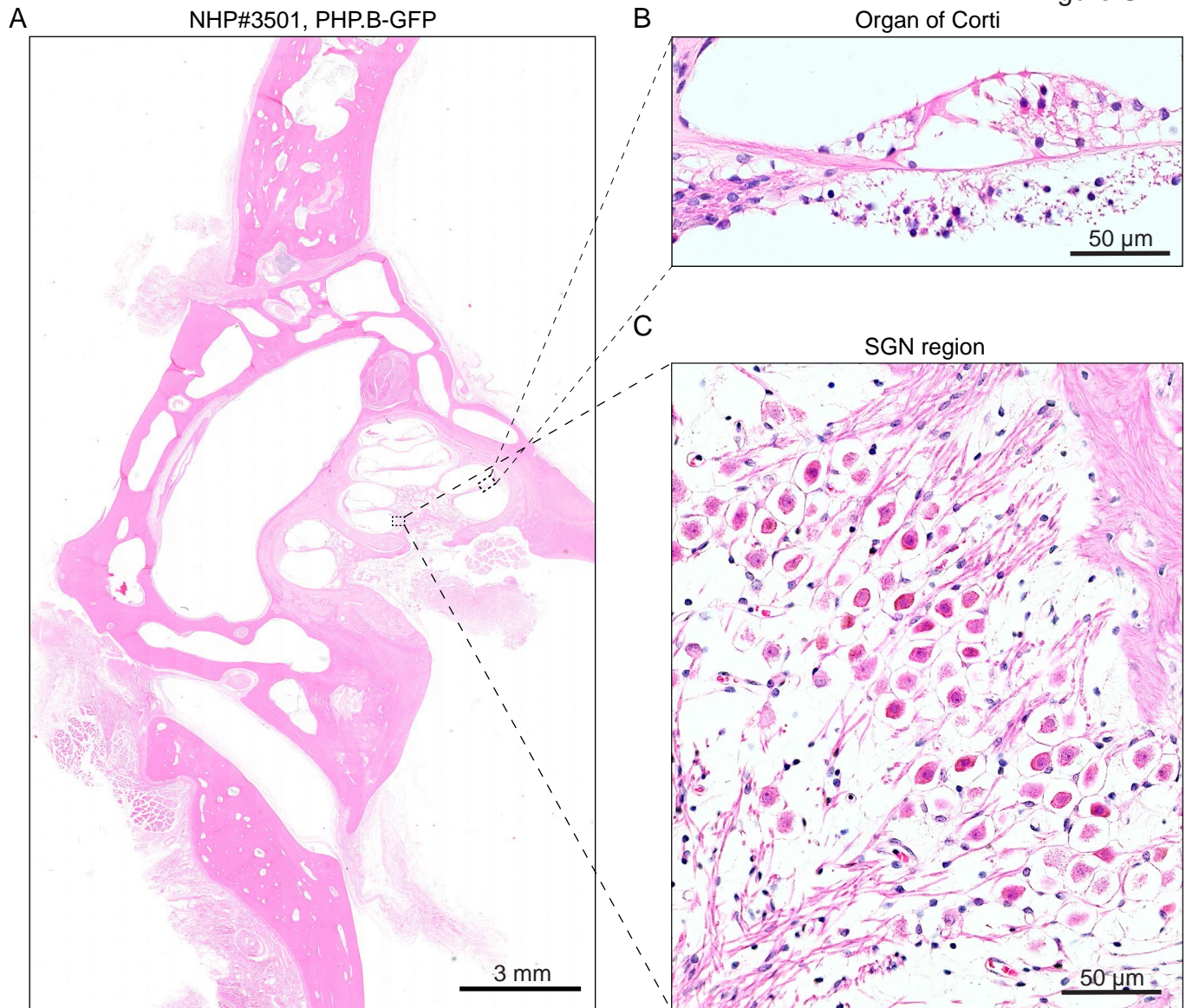


Figure S17. Hematoxylin and Eosin staining of the AAV9-PHP.B-CBA-GFP (1×10^{11} VG) left injected ear of Cynomolgus monkey #3501. (A) A low magnification image is shown with areas of interest indicated by rectangles. (B) Magnified image of organ of Corti and (C) spiral ganglion neurons (SGN) region.

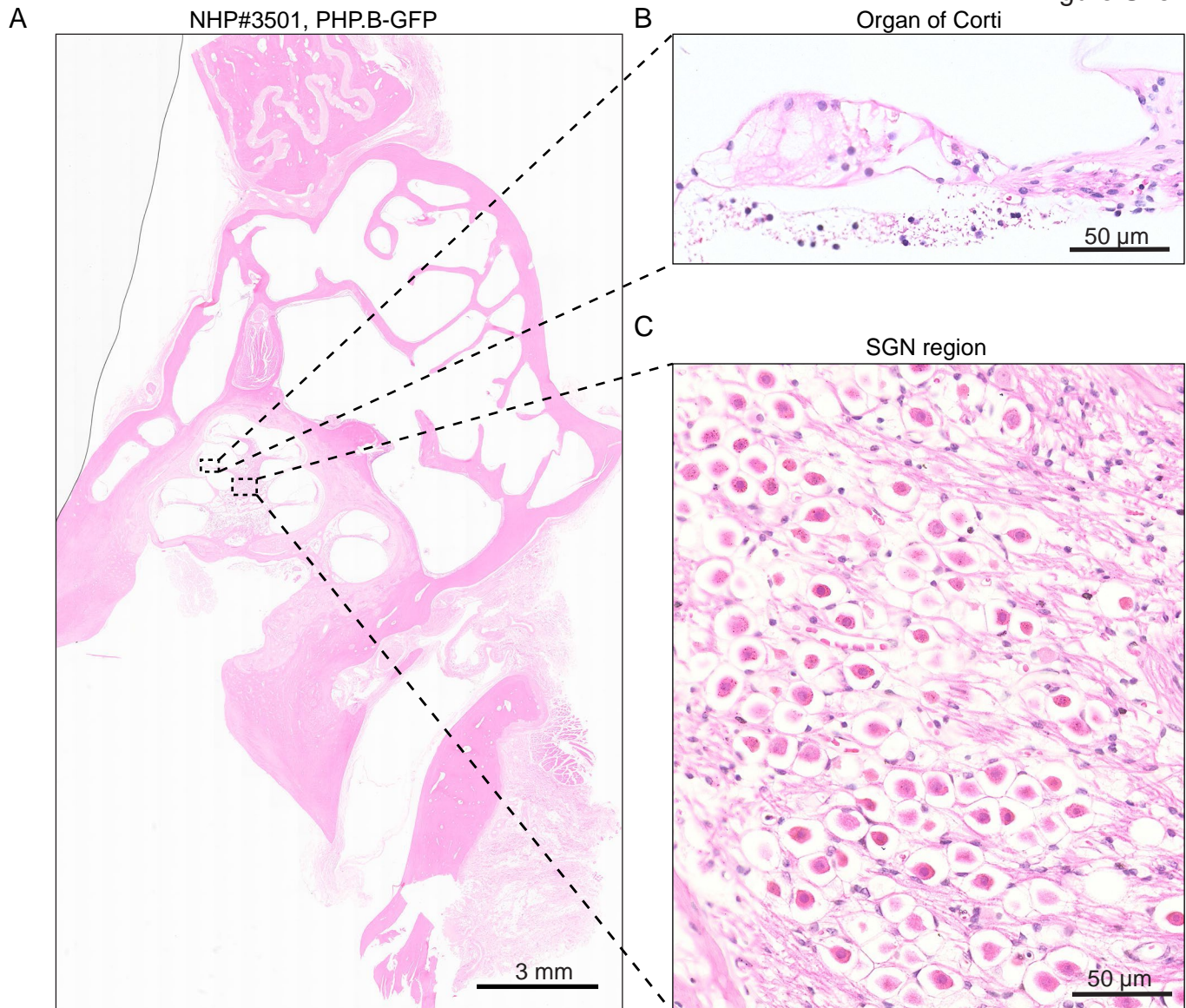


Figure S18 Hematoxylin and Eosin staining of the AAV9-PHP.B-CBA-GFP (1×10^{11} VG) right injected ear of Cynomolgus monkey #3501. (A) A low magnification image is shown with areas of interest indicated by rectangles. (B) Magnified image of organ of Corti and (C) spiral ganglion neurons (SGN) region.

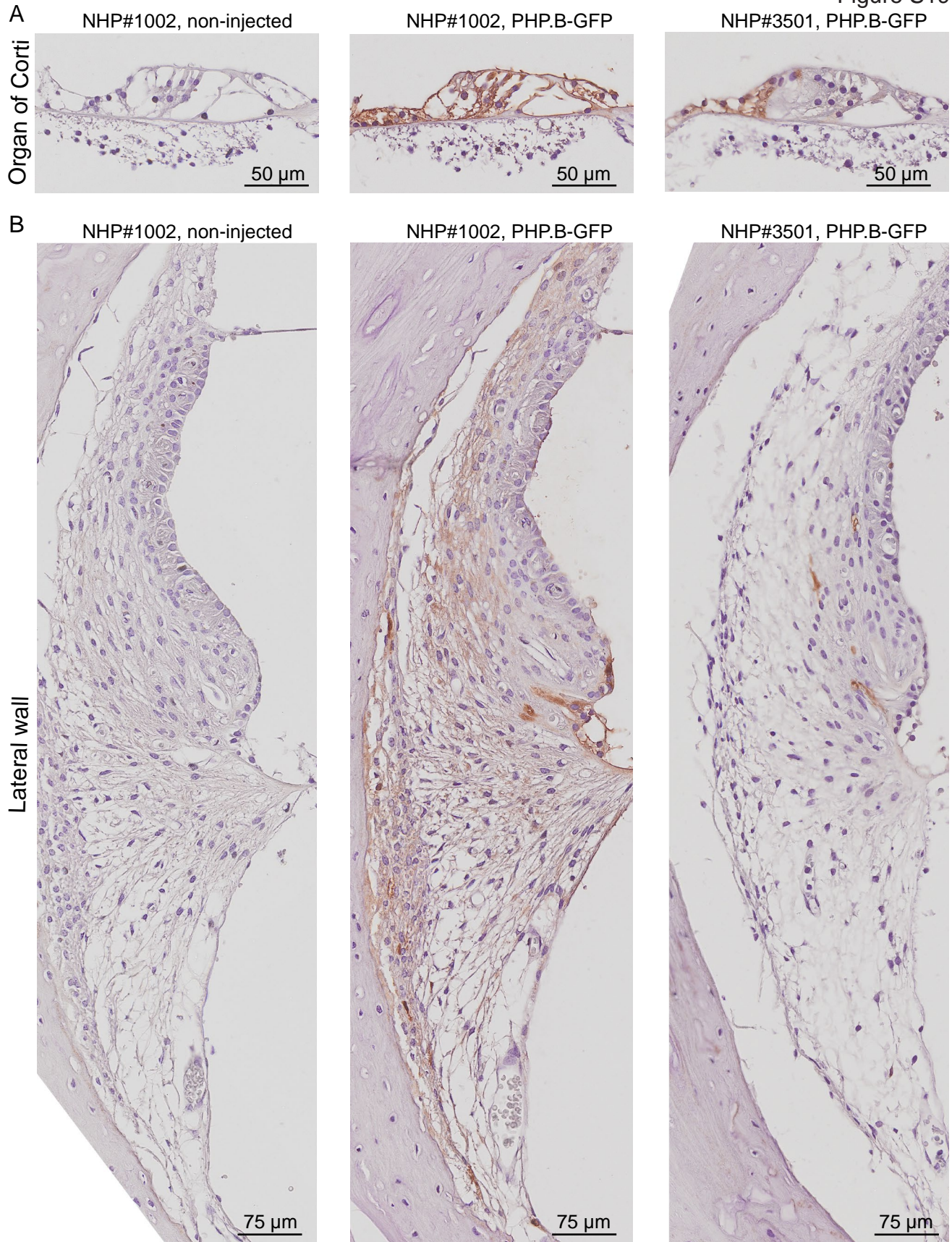


Figure S19. Transduction profile of AAV9-PHP.B-CBA-GFP in the organ of Corti and lateral wall of Cynomolgus monkeys #1002, injected with AAV9-PHP.B-CBA-GFP (3×10^{11} VG) and #3501, injected with AAV9-PHP.B-CBA-GFP (1×10^{11} VG). **(A)** Organ of Corti of non-injected ear (left) and injected ear (middle) of Cynomolgus monkey #1002 and injected ear (right) of Cynomolgus monkey #3501. **(B)** The lateral wall of non-injected ear (left) and injected ear (middle) of Cynomolgus monkey #1002 and injected ear (right) of Cynomolgus monkey #3501.